

Supporting information for review

Electrical and Thermal Properties of a Carbon Nanotube/Polycrystalline BiFeO₃/Pt Photovoltaic Heterojunction with CdSe Quantum Dots Sensitization

Yongyuan Zang,¹⁾ Dan Xie,²⁾ Yu Chen,²⁾ Tianling Ren,²⁾ Hongwei Zhu^{3,4)} and David Plant¹⁾

¹⁾Electrical and Computer Engineering, McGill University, Montreal, Quebec, H3A 2T8, Canada

²⁾Institute of Microelectronics, Tsinghua University, Beijing, 100084, P. R. China

³⁾Key Laboratory for Advanced Manufacturing by Material Processing Technology and Department of Mechanical Engineering, Tsinghua University, Beijing 100084, P. R. China

⁴⁾Center for Nano and Micro Mechanics (CNMM), Tsinghua University, Beijing 100084, P. R. China

This supplementary information section is designed in the form of Q&A. Due to paragraph constraints, most of the current and voltage expressions are given directly. A detailed derivation process is provided in this supplementary material.

Content

Q-1: How is the energy band diagram of the CNT/BFO/Pt heterojunction constructed?

Q-2: How is the equivalent electrical model constructed, and how is the dark current density calculated?

Q-3: How is the photocurrent current density calculated?

Q-4: How does thermal modulation impact the photovoltaic properties?

Q-1: How is the energy band diagram of the CNT/BFO/Pt heterojunction constructed?

Answer:

To construct the band diagram, the band gap (E_g) and electron affinities (χ) of BFO are estimated to be 2.2 and 3.3 eV, respectively. The work function (Φ) of CNT and Pt are taken as 4.8 and 5.6 eV, respectively. When BFO and CNT or Pt are joined, two Schottky barriers will be formed with two built-in fields in opposite directions. The two interface junctions are both depleted.

The width of depletion region (x_{dc}) can be given as follows:

$$x_{dc} = \sqrt{\frac{2\varepsilon_0\varepsilon_s V_s}{qN_D}}, \quad (1)$$

where, ε_0 is the vacuum permittivity, ε_s is the relative dielectric constant of the BFO material,

N_D is the carriers density, V_s is the surface potential and can be defined as:

$$V_s = V_{x=surface} - V_{x=x_{dc}}, \quad (2)$$

which can be used to describe the potential barrier difference between surface and body, and represents the band bending.

By calculating the widths of the depletion regions at both the CNT/BFO and BFO/Pt sides, it can be found that the entire width of the two depletion regions (~ 500 nm) is larger than the BFO thickness (~ 300 nm) in the experiment. Thus, the entire BFO thin film is depleted across the top and bottom electrodes without any neutral region.

Therefore, the modified Poisson Equation can be applied at both interfaces of GNTs/BFO and BFO/Pt:

$$\frac{d^2V(x)}{dx^2} = -\frac{1}{\varepsilon_0\varepsilon_s} \left(\rho(x) - \frac{dP_r(x)}{dx} \right), \quad (3)$$

where $V(x)$ is the voltage potential, $\rho(x)$ is the charge density, and $P_r(x)$ is the remnant polarization. The variable $\rho(x)$ can be determined as follows:

$$\rho(x) = q[p_D(x) + p(x) - n_A(x) - n(x)], \quad (4)$$

where $n(x)$ and $p(x)$ are the electron and hole density, respectively. $n_A(x)$ and $p_D(x)$ are the ionized donor and acceptor density, respectively. Here, we can assume that electrons and holes can be described by the Fermi Distribution:

$$\left. \begin{aligned} n(x) &= n_0 e^{qV(x)/K_B T} \\ p(x) &= p_0 e^{-qV(x)/K_B T} \end{aligned} \right\} \quad (5)$$

where n_0 and p_0 are the electron and hole density at thermal equilibrium. Also, $n_0 \approx N_D$,

and K_B is the Boltzmann constant.

When the electro neutrality condition $q[p_D + p_0 - n_A - n_0] = 0$ is met:

$$p_D - n_A = n_0 - p_0. \quad (6)$$

For completeness, it is noted that:

$$\frac{qV(x)}{K_B T} = u(x). \quad (7)$$

Therefore, Eq. (4) can be written as:

$$\rho(x) = q[p_0(e^{-u} - 1) - n_0(e^u - 1)]. \quad (8)$$

For BFO, $n_0 \gg p_0$, so (6) can be simplified as follows:

$$\rho(x) = -qn_0(e^u - 1). \quad (9)$$

$P_r(x)$ can be calculated by:

$$P_r(x) = \frac{P_{r\max}}{E_{c\max}} E_c(x), \quad (10)$$

where $P_{r\max}$ and $E_{c\max}$ represent the remnant polarization and the coercive field in the saturated polarization-electric field (P - E) hysteresis loop, respectively, and E_c is the electric field.

Therefore, Eq.(3) can be given as,

$$\frac{d^2V(x)}{dx^2} = \frac{1}{\epsilon_0\epsilon_s} [qn_0(e^u - 1) + \frac{dP_r(x)}{dx}]. \quad (11)$$

Using the Taylor expansion,

$$e^u - 1 = u + \frac{u^2}{2} + \dots + \frac{u^n}{n!} + \dots,$$

Eq.(10) can be solved subsequently.

N.B. boundary conditions can be given when interface states are taken into consideration during the derivation process, as follows:

$$\left. \begin{aligned} V(L) &= V_{sBFO-Pt} \\ V(0) &= V_{sCNT-BFO} \end{aligned} \right\}, \text{ where } L \text{ is the thickness of the BFO thin film, and } V_{sCNT-BFO} \text{ and}$$

$V_{sBFO-Pt}$ are the surface potentials at CNT/BFO and BFO/Pt, respectively.

By applying the boundary conditions, three possible schematic energy band diagrams of the CNT/BFO/Pt heterojunction can be simulated in MATLAB®, and are shown in Figs. 1-3.

(A) *Double depleted*

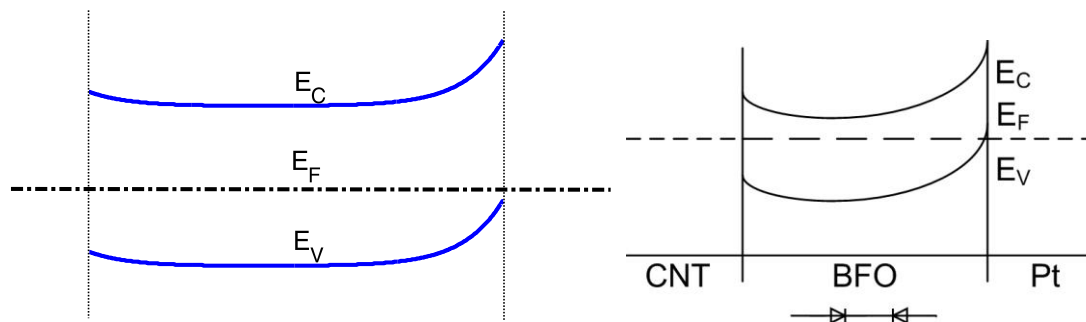


FIG.1. Depletion regions are formed on both sides. Such a band diagram is equivalent to two back-to-back diodes, and no current will be observed regardless of if the applied voltage is positive or negative.

(B) *Upward bending*

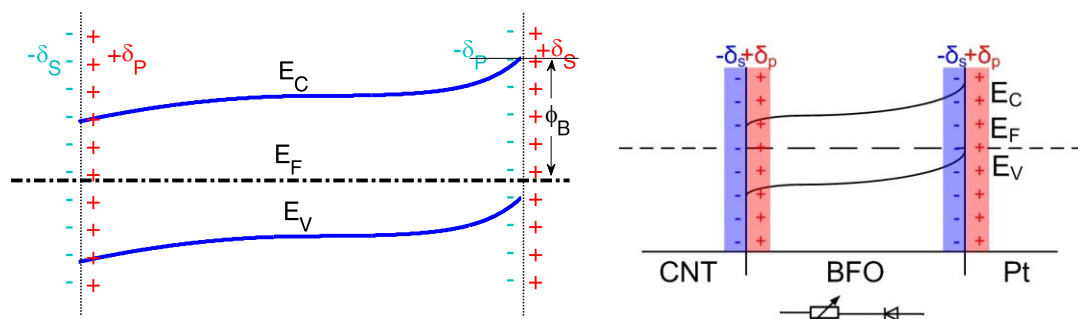


FIG.2. Electrons are accumulated at the CNT/BFO side and can be regarded as a variable resistance; and the BFO/Pt side is depleted and can be treated as a Schottky diode.

(C) *Downward bending*

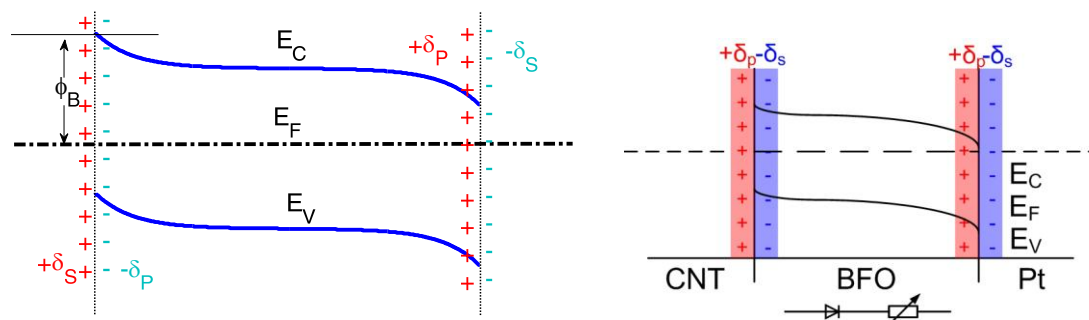


FIG.3. Electrons are accumulated at BFO/Pt side and can be regarded as a variable resistance; and the CNT/BFO side is depleted and can be treated as a Schottky diode.

Q-2: How is the equivalent electrical model constructed, and how is the dark current density calculated?

Answer:

As explained in the paper, interface trapped charges and a high enough electric field will switch the ferroelectric polarization in the BFO thin film and stimulate neutral oxygen vacancy to release electrons, forming a narrow electron region near the interface and resulting in the energy band bending in the application.

When a positive electrode is connected to a Pt electrode, a depletion region will be formed at the BFO/Pt side, as shown in Fig.2.

When the diffusion model dominates, the current density can be written as,

$$j = q\mu_n EN_c e^{-\frac{q\Phi_B}{k_B T}} (e^{\frac{qV_F}{k_B T}} - 1) \quad (12)$$

where μ_n is the mobility of electrons, $N_c = 2\left(\frac{m_{dn} k_B T}{2\pi\hbar^2}\right)^{3/2}$ is the equivalent density of states at the bottom of the conduction band, m_{dn} is the effective mass of an electron, Φ_B is the built-in potential, and V_F is the junction bias. E is the electrical field of space charge region, and can be defined as,

$$E = \sqrt{\frac{2qN_D(\phi_i - V_F)}{\epsilon_0 \epsilon_s}}, \quad (13)$$

where $\phi_i = (E_{Cx=surf} - E_{Cx=x_{dc}}) / q$ represents the band bending.

When the thermal emission model dominates, the current density can be written as,

$$j = A^* T^2 e^{-\frac{q\Phi_B}{k_B T}} (e^{\frac{qV_F}{k_B T}} - 1), \quad (14)$$

where $A^* = 4\pi q m_{dn} k_B^2 / h^3$ is the Richardson constant.

In the experiment, a sol-gel process is used to prepare the BFO thin film and both of the two models should be taken into account in the modeling. Thus the optimized current density can be described as,

$$j = \frac{q\bar{v}N_v}{4 + \frac{\bar{v}}{v_D}} e^{-\frac{q\Phi_B}{k_B T}} (e^{\frac{qV_F}{k_B T}} - 1), \quad (15)$$

where $\bar{v} = \left(\frac{8k_B T}{\pi m_n}\right)^{1/2}$ is the average thermal velocity, $v_D = \mu_n E$ is the carrier drift velocity,

and μ_n is the mobility of electrons.

Electrons are accumulated at the CNT/BFO side and can be modeled as a variable resistance,

$$\sigma = qp\mu_p + qn\mu_n \approx qn\mu_n, \quad (16)$$

a value which can be regarded as constant. The width of depletion region will change with different external applied voltages, and the resistance will vary as follows:

$$R = \frac{1}{\sigma}(L - x_{dc}). \quad (17)$$

When a positive electrode is connected to the CNT electrode, a depletion region will be formed at the CNT/BFO side, as shown in Fig.3, and a similar analysis as above can be applied.

The equivalent electrical model, provided in Fig.4, can be obtained based on this analysis.

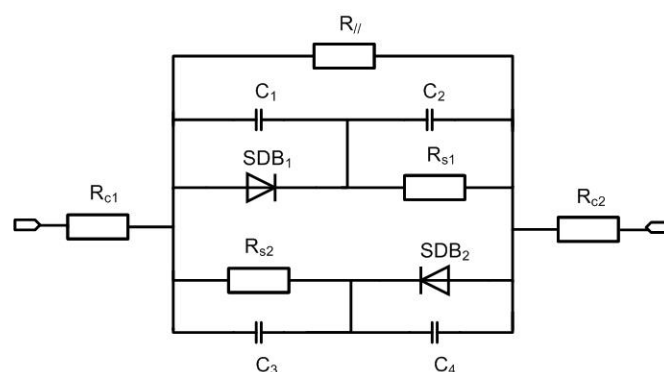


FIG4. Equivalent electrical model

In Fig.4, SDB_1 and SDB_2 are the Schottky barrier diodes, R_{s1} and R_{s2} are the variable resistances, R_{c1} and R_{c2} are the contact resistances with the CNT and Pt electrodes, $R_{//}$ is the edge resistance caused by imperfect factors, and C_1 to C_4 are junction capacitances.

According to this electrical model, the short circuit current should be zero with illumination. However, interface trapped charges offer a weak ferroelectric polarization δ at the interface, leading to a weak band bending and sub on-state of the diode at zero bias, resulting in a non-zero dark current. Therefore, a voltage source V_{sub} is added to characterize I - V curve offset at zero bias.

Moreover, the electrical model should be “dynamic” in a practical application. The parameters of the SDB_1 and SDB_2 such as the width of the depletion region, potential barrier height, and so forth, will vary with different applied voltages. In order to simplify our model, the parameters of SDB_1 and SDB_2 are set with an approximation, and a current supply J_R is introduced to describe such circuit parameter induced current variation and leakage terms in the heterojunction. The modified equivalent electrical model is given in Fig.5.

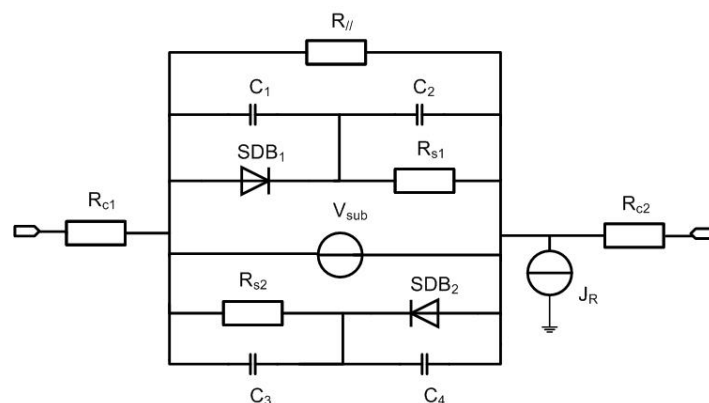


FIG.5. Modified equivalent electrical model

The relationship between the dark current density and device bias is given as:

$$j = j_{dark_model}(V). \quad (18)$$

Q-3: How is the photocurrent current density calculated?

Answer:

The photo current under illumination can be described as follows:

$$I = I_L - I_F = A_E j_L - A_T j_{dk}(V), \quad (19)$$

where A_E is the illumination area, A_T is the cell area, j_L is photocurrent density, and j_{dk} is the dark current density. The dark current density can be obtained from the electrical model, giving $j_{dk}(V) = j_{dark_model}(V)$.

The photo current density j_L can be estimated as follows:

$$j_L = q \int_0^\infty \int_0^{x_{dc}} \beta \Phi_0(\lambda) [1 - \rho(\lambda)] \alpha e^{-\alpha x} dx d\lambda, \quad (20)$$

where β is the generation coefficient, Φ_0 is the intensity of a photon with wavelength λ , ρ is the reflectance, and α is the absorption coefficient.

As is explained in the paper, the location of the depletion region will change with different applied voltages. It is on the BFO/Pt side under forward bias and switches to the CNT/BFO side with reverse bias. Since the potential barrier is higher at the BFO/Pt side compared with the CNT/BFO side, a larger built-in electric field will be formed and thus a larger photocurrent

density will be achieved with the forward bias situation; this serves as the reason for the I - V curve's asymmetry, and is also why a larger current density can be found in the forward bias.

The short circuit current under illumination (I_{sc}) can be given as follows:

$$I_{sc} = I_L(0) - I_F(0). \quad (21)$$

Similarly, the open circuit voltage (V_{oc}) can be calculated from:

$$I = I_L(V_{oc}) - I_F(V_{oc}) = 0. \quad (22)$$

Q-4: How does thermal modulation impact the photovoltaic properties?

Answer:

To explain the effect that thermal modulation has on the photovoltaic effect, the thermionic emission model should be employed as the principal factor, as illustrated in Eq.(16).

For a simple case, where impacts introduced by resistance and capacitance are omitted, the photocurrent density under forward bias can be written as:

$$j = A^* T^2 e^{-\frac{q\Phi_B}{K_B T}} \left(e^{\frac{q(V_F - V_{sub})}{K_B T}} - 1 \right) - j_R \sim A^* T^2 e^{-\frac{q\Phi_B}{K_B T}} e^{\frac{q(V_F - V_{sub})}{K_B T}} - j_R. \quad (23)$$

The short circuit current under heating can be obtained from:

$$j_{sc} = A^* T^2 e^{-\frac{q\Phi_B}{K_B T}} e^{-\frac{-qV_{sub}}{K_B T}} - j_R. \quad (24)$$

It can be concluded that the photocurrent should exhibit a parabolic growth with T in the low temperature region. However, both experimental results and simulated curves at low temperatures exhibit a linear variation. The junction bias variation under different temperatures is a principal contributing factor to this effect. In Eq.(16), the junction bias V_F is considered to be constant in the simulation. However, the photocurrent increases as temperature increases, leading to a larger voltage drop over the resistance, and thus less bias will be applied to the junction. Incorporating the junction bias decreases into Eq.(16), the photocurrent would vary linearly with different operating temperatures.

To calculate the open circuit voltage (V_{oc}),

$$j_{sc} = A^* T^2 e^{-\frac{q\Phi_B}{K_B T}} e^{\frac{q(V_{oc} - V_{sub})}{K_B T}} - j_R = 0. \quad (25)$$

Therefore, V_{oc} can be approximated as follows:

$$V_{oc} = \frac{K_B T}{q} (\ln j_R - \ln A^* - 2 \ln T) + V_{sub} + \Phi_B; \quad (26)$$

since $\ln j_R - \ln A^* - 2 \ln T < 0$, V_{oc} decreases as T increases in the low temperature region.